# Appendix A Supporting information

## Organocatalyzed ring opening polymerization of lactide from the surface of cellulose nanofibrils

Michael Lalanne-Tisné[ab], Maarten A. Mees[a], Samuel Eyley[a], Philippe Zinck[b*], Wim Thielemans[a*]

a. Sustainable Materials Lab, Department of Chemical Engineering, KU Leuven, Campus Kulak Kortrijk, Etienne Sabbelaan 53, box 7659, B-8500 Kortrijk, Belgium

*wim.thielemans@kuleuven.be

b. Univ. Lille, CNRS, Centrale Lille, ENSCL, Univ. Artois, UMR 8181 - UCCS - Unité de Catalyse et Chimie du Solide, F-59000 Lille, France

*philippe.zinck@univ-lille.fr

Corresponding author:

Prof. Dr. Ir. Wim Thielemans FRSC
Provincial Chair of Advanced Materials
Sustainable Materials Laboratory
Science and Technology
KU Leuven Campus Kortrijk
Etienne Sabbelaan 53
8500 Kortrijk
Belgium

Phone: +32 (0)56 24 61 71
Fax: +32 (0)56 24 69 97

# 1. Table of Contents

## S1. Characterization method of modified CNF

Elemental composition (C, H, N, and S) of modified CNFs after purification was measured with a Thermo Scientific FLASH 2000 elemental analyzer, using about 1 mg of dry sample each time. The standard used for calibration was 2,5-Bis(5-tert-butyl-2-benzo-oxazol-2-yl)thiophene (BBOT) provided by Elemental Microanalysis (UK). Vanadium pentoxide $V_2O_5$ was used to help in sulphur determination. All the values reported are the average of 3 measurements for each sample.

A Netzsch TG 209 F3 Tarsus was use to carry out thermogravimetric analysis (TGA). Samples of around 2 mg were placed in aluminum-(III)-oxide pans and heated from 30 to 600°C at a ramp rate of 10°C/min under argon flow. Water content of the various samples was determined as the difference between the initial mass and the stabilized mass around 100°C. The determined water content was taken into account in the determination of the level of surface modification based on elemental composition results in line with our earlier reported procedure[(1)].

Infrared spectra of CNF were measured using a Bruker ALPHA FT-IR spectrophotometer to determine the success of the reaction on the CNF. The measurements were carried out in attenuated total reflection (ATR) mode. Spectra were acquired as the sum of 16 scans over a frequency ranging from 4000 to 400 $cm^{-1}$ on CNF deposited onto the spectrophotometer.

Surface-sensitive analysis of modified CNF was carried out by X-ray photoelectron spectroscopy (XPS) on a Kratos Axis Supra photoelectron spectrometer using a monochromated Al Kα ($h\nu$ = 1486.7 eV, 5 mA) X-ray source, hybrid (magnetic/electrostatic) optics, and a hemispherical analyzer with a pass energy of 160 eV for survey spectra and 20 eV for high resolution spectra. Spectra were acquired under charge neutralization conditions using an electron flood gun within the field of the magnetic lens. Spectra were charge corrected to aliphatic carbon at 285.0 eV. Spectra were processed in CasaXPS with Tougaard 2-parameter backgrounds used for integration and LA(α, m) lineshapes corresponding with a Voigtian function with Lorentzian exponent α and Gaussian width m used for fitting high resolution spectra. Empirical relative sensitivity factors supplied by Kratos Analytical (Manchester, UK) were used for quantification.

The number-average molecular weight (Mn) and the dispersity (Đ) of extracted PLA homopolymer by soxhlet extraction were determined by Size Exclusion Chromatography (SEC) in tetrahydrofuran at 40 °C at a flow rate of 1 $mL.min^{-1}$. Mn and Đ were determined from the Refractive Index (RI) signal using a calibration curve based on polystyrene (PS) standards from Polymer Standards Service, on a Waters apparatus equipped with Waters Styragel columns HR2, HR3, HR5 and HR5E.

$^{1}$H NMR spectra were recorded on AVANCE III HD 300 Bruker spectrometer (7.1 Tesla) at room temperature in deuterated dimethyl sulfoxide (0.6 ml) for the crude mixture, as well as DMAP and DL-Lactide separately.

References:

(1) Eyley, S., Schütz, C., & Thielemans, W. (2018). Surface Chemistry and Characterization of Cellulose Nanocrystals. In T. Rosenau, A. Potthast, & J. Hell (Eds.), *Cellulose Science and Technology* (pp. 223–252). John Wiley & Sons, Inc.

## S2. Elemental analysis result treatment

Calculation method used with elemental analysis result is done with a script taking into account the content of the unmodified cellulose, its water content as determined by TGA, and compares the elemental analysis result for the modified CNF. Both EA and TGA are run in parallel to obtain an accurate value of the quantity of water present in the sample that is analyzed in EA. As all the analysis could not be done at the same time, the starting cellulose was run through EA and TGA again for every series of measurement to obtain more accurate results when comparing with the modified cellulose samples.

Below is an example of what the script returns when EA and TGA parameters are inputted.

*Table 1: parameters measured by elemental analysis and TGA, to be inputted in the script calculating the w% amount of polymer grafted on cellulose*

| | | **Unmodified CNF** | **MLT6-3 (entry 15)** |
|---|---|---|---|
| Found | **C** | 42.424 | 44.070 |
| | **H** | 6.111 | 6.074 |
| % adsorbed water | | 2.73 | 2.48 |

Nitrogen content was measured, but only very small traces were present, with values around the detection limit for the measuring device, and modified cellulose presented on average a similar amount of Nitrogen compared to the starting CNF, therefore it was considered negligible in the calculation. Sulfur was not seen in the analysis, unlike modification done on cellulose nanocrystals which can show traces element of sulfur due to the use of sulfuric acid in the preparation of CNC.

The method used to determine grafting weight % uses the known elemental composition of lactide (through chemical formula) and of unmodified cellulose nanofibrils (by elemental analysis) to determine the result of a an equation that leads to the weight % that is attributed to grafting in the sample.

The calculation therefore is similar to solving this kind of equation:

$\%C_{sample} = \%C_{PLA}.x + \%C_{CNF}$
.(1-x) ; with x being the weight % of PLA
The script used is however more complicated, as it also takes into account the mass % of hydrogen measured during elemental analysis and corrects all values by including water contribution, along with minimizing some other factors.

Below is an example of the information returned by the script when entering the elemental composition and water content of the starting material and the modified one.

6-3

%run C:\Users\u0127675\Desktop\Data\Elemental_analysis\EA_calculator_polymer_grafting.py 44.070 6.074 2.48 --celC 42.424 --celH 6.111 --celwater 2.73 \ --polyC 3 --polyH 4 --polyO 2

```
[[Fit Statistics]]
    # fitting method   = Nelder-Mead
    # function evals   = 26
    # data points      = 5
    # variables        = 1
    chi-square         = 1.7716e-13
    reduced chi-square = 4.4290e-14
    Akaike info crit   = -152.855832
    Bayesian info crit = -153.246394
 [[Variables]]
    cel:    0.75721708 (init = 0.6)
    total:  1 (fixed)
    poly:   0.24278292 == 'total-cel'
    water:  0.0248 (fixed)
Calculated: C, 45.17; H, 5.88; O, 0; N, 0.0; S, 0.0%
Found (water corrected): C, 45.19; H, 5.94; O, 0; N, 0.0; H, 0.0%
Mass Fraction cellulose: 0.76
Mass Fraction grafted polymer: 0.24
Corrected for product water content of: 2.48%
Corrected for starting material water content of: 2.73%
```

Below are compiled tables of the samples described in the publication with their EA and TGA data.

*Table 2: EA and TGA data obtained for samples using freeze dried cellulose and their calculated PLA content*

| Sample | Carbon content (%) | Hydrogen content (%) | Water content (%) | Grafted PLA (wt%) |
|---|---|---|---|---|
| **1** | 41.71 | 5.78 | 2.42 | 6 |
| **2** | 41.61 | 5.77 | 2.65 | 6 |
| **3** | 41.78 | 5.80 | 2.54 | 8 |
| **4** | 41.47 | 5.83 | 3.24 | 8 |
| **5** | 42.01 | 5.77 | 2.53 | 11 |
| **6** | 43.01 | 5.77 | 1.60 | 19 |
| **7** | 41.95 | 5.68 | 2.90 | 12 |
| **8** | 42.56 | 5.74 | 2.30 | 17 |

*Table 3: EA and TGA data obtained for samples using never-dried cellulose and their calculated PLA content. a: experiment done using freeze-dried cellulose instead.*

| *Entry* | *Carbon content (%)* | *Hydrogen content (%)* | *Water content (%)* | *Grafted PLA (wt%)* |
|---|---|---|---|---|
| ***1*** | 41.83 | 6.08 | 4.40 | 7 |
| ***2*** | 41.87 | 6.09 | 3.48 | 13 |
| ***3*** | 41.62 | 6.05 | 4.78 | 7 |
| ***4*** | 43.69 | 6.18 | 2.47 | 18 |
| ***5*** | 42.49 | 6.13 | 3.60 | 16 |
| ***6*** | 41.36 | 5.98 | 4.05 | 5 |
| ***7*** | 42.11 | 6.03 | 2.97 | 9 |
| ***8*** | 42.16 | 6.08 | 3.60 | 11 |
| ***9*** | 41.98 | 6.16 | 3.62 | 9 |
| ***10*** | 42.13 | 6.19 | 3.89 | 12 |
| ***11*** | 40.27 | 5.94 | 5.87 | 6 |
| ***12*** | 43.55 | 6.21 | 2.77 | 17 |
| ***13*** | 43.01 | 6.05 | 1.65 | 12 |
| ***14*** | 42.28 | 6.17 | 3.39 | 18 |
| ***15*** | 44.07 | 6.07 | 2.48 | 24 |
| ***16[a]*** | 42.15 | 5.88 | 4.55 | 13 |

## S3. FT-IR data

Typical FT-IR spectra will be analyzed here, with details provided about noticeable peaks for both modified and non-modified cellulose nanofibrils.

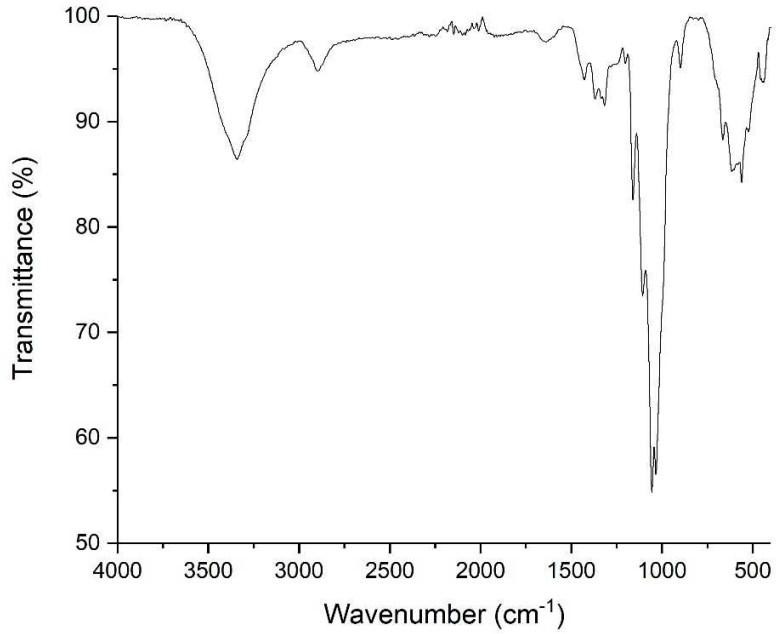


*Figure 1: FT-IR spectra of dried, unmodified cellulose nanofibrils recorded in ATR mode*

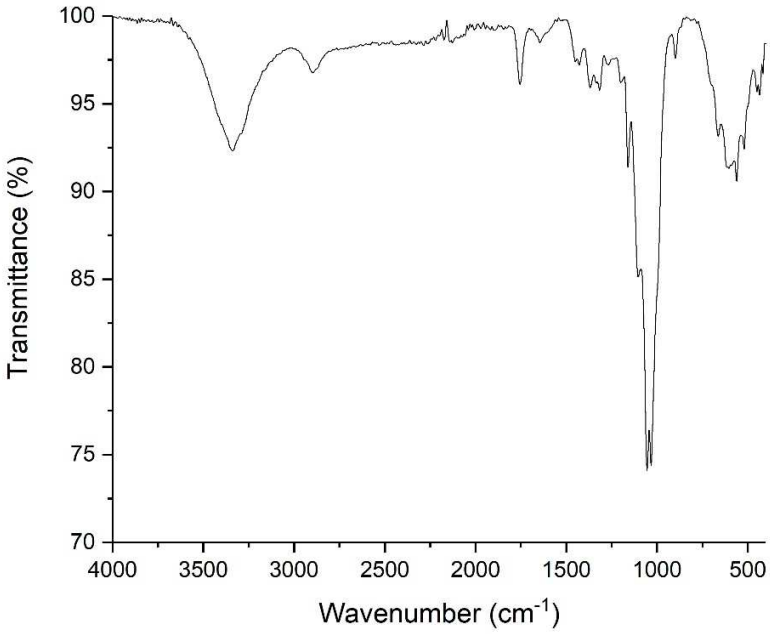


*Figure 2: FT-IR spectra of dried, modified cellulose nanofibrils from freeze dried cellulose recorded in ATR mode*

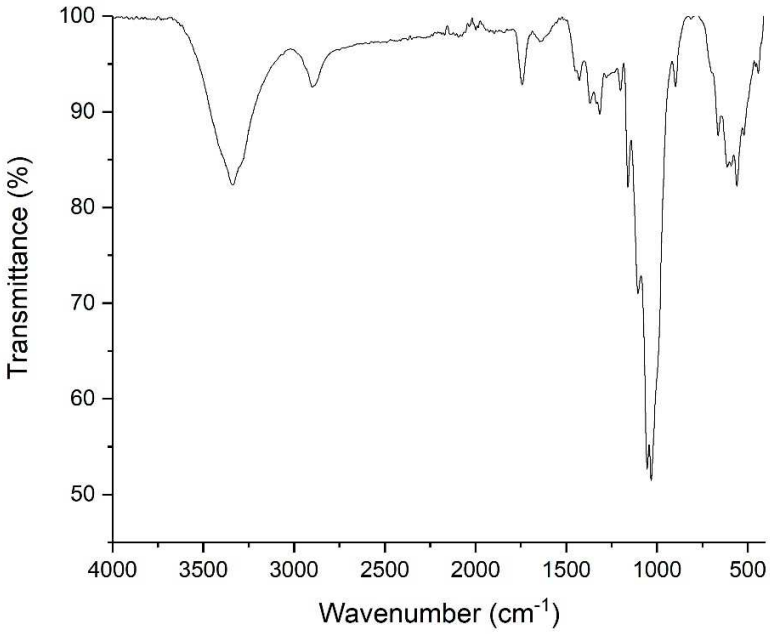


*Figure 3: FT-IR spectra of dried, modified cellulose nanofibrils from never-dried cellulose recorded in ATR mode*

*Table 4: FTIR signals detected for unmodified and modified CNFs, with their corresponding functions*

| **bond** | **wave number $cm^{-1}$ unmodified CNF** | **wave number $cm^{-1}$ modified CNF** |
|---|---|---|
| ν (O-H) | 3342 | 3335 |
| ν (C-H) | 2899 | 2899 |
| ν (C=O) | | 1743 |
| δ ($H_2O$) | 1639 | 1646 |
| δ (C-O-H) | 1428 | 1428 |
| δ (C-O-H) | 1369 | 1369 |
| δ (C-O-H) | 1317 | 1316 |
| ν (C-O, ester) | | 1201 |
| ν (C-O-C, glucose ring asym.) | 1160 | 1160 |
| ν (C-OH) | 1107 | 1105 |
| ν (C-OH) | 1056 | 1055 |
| ω (C-OH) | 665-561 | 663-560 |

## S5. NMR Spectra

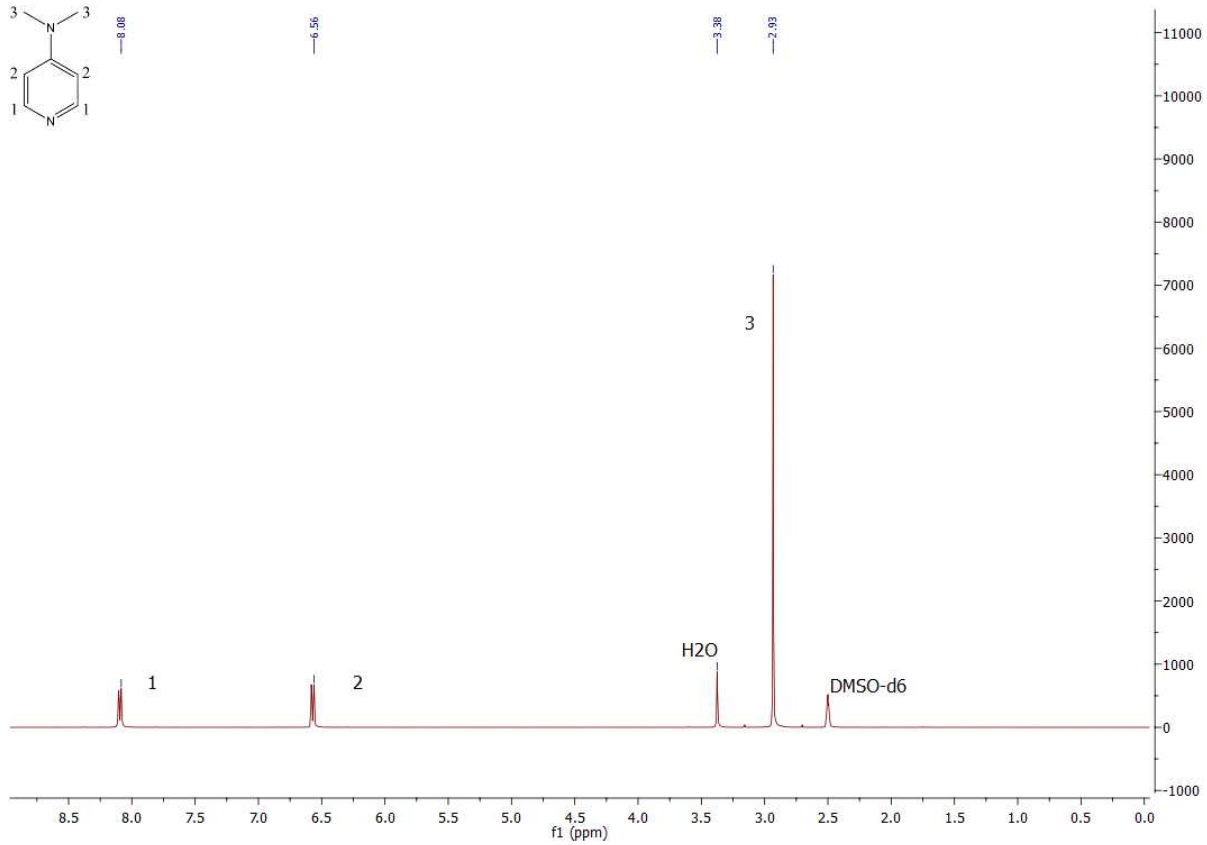


*Figure 4: 1H NMR spectra of N,N-Dimethylpyridin-4-amine in DMSO-d6*

$^{1}$H NMR (DMSO-d6, 300 MHz) δ (ppm) 8.08 (d, 2H), 6.56 (d, 2H), 2.93 (s, 6H)

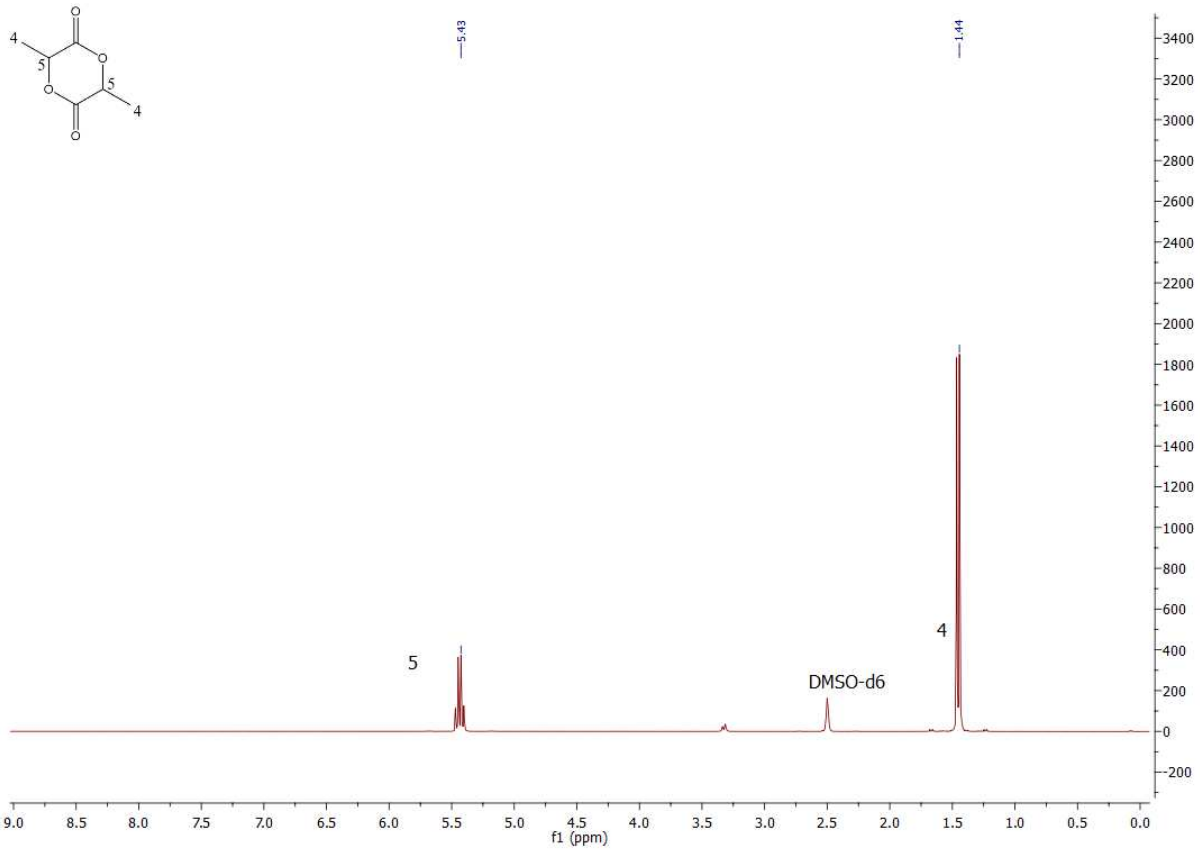


*Figure 5: 1H NMR spectra of DL-Lactide in DMSO-d6*

$^{1}$H NMR (DMSO-d6, 300 MHz) δ (ppm) 5.43 (q, 2H), 1.44 (d, 6H)

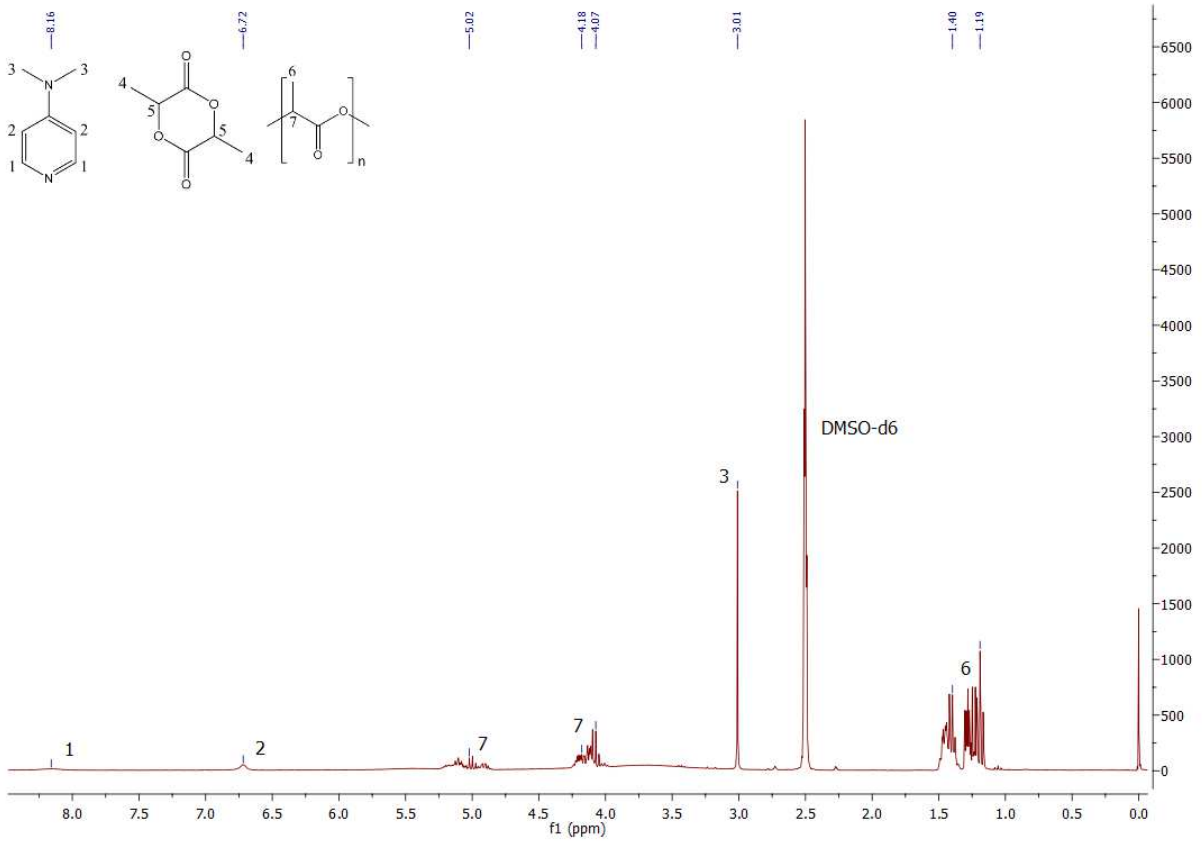


*Figure 6: 1H NMR spectra of crude mixture after reaction in DMSO-d6. Corresponds to entry 3 in table 3 (table 2 in the main manuscript)*

$^{1}$H NMR (DMSO-d6, 300 MHz) δ (ppm) 8.16 (s, 2H), 6.72 (s, 2H), 4.86-5.21 (m, 1H), 4.10-4.24 (m, 1H), 3.01 (s, 6H), 1.16-1.49 (m, 3H)

Due to the presence of oligomers, the signals for proton 6 and 7 are split into two multiplet that are quite distinct, are they are many chain ends. The same phenomenon can be observed for the other NMR that have been performed on the crude mixture. The presence of short oligomers was also confirmed by size exclusion chromatography.

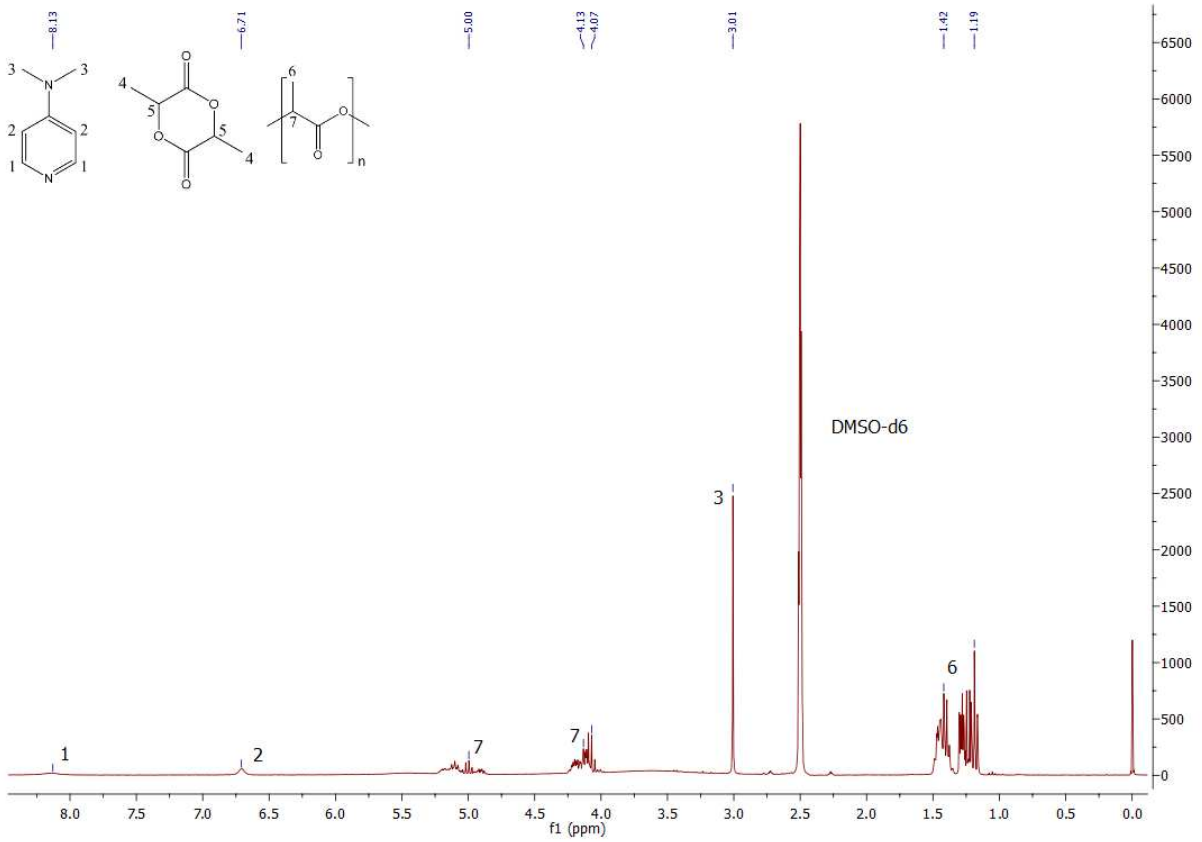


*Figure 7: 1H NMR spectra of crude mixture after reaction in DMSO-d6. Corresponds to entry 8 in table 3 (table 2 in the main manuscript)*

$^{1}$H NMR (DMSO-d6, 300 MHz) δ (ppm) 8.13 (s, 2H), 6.71 (s, 2H), 4.85-5.22 (m, 1H), 4.10-4.23 (m, 1H), 3.01 (s, 6H), 1.16-1.49 (m, 3H)

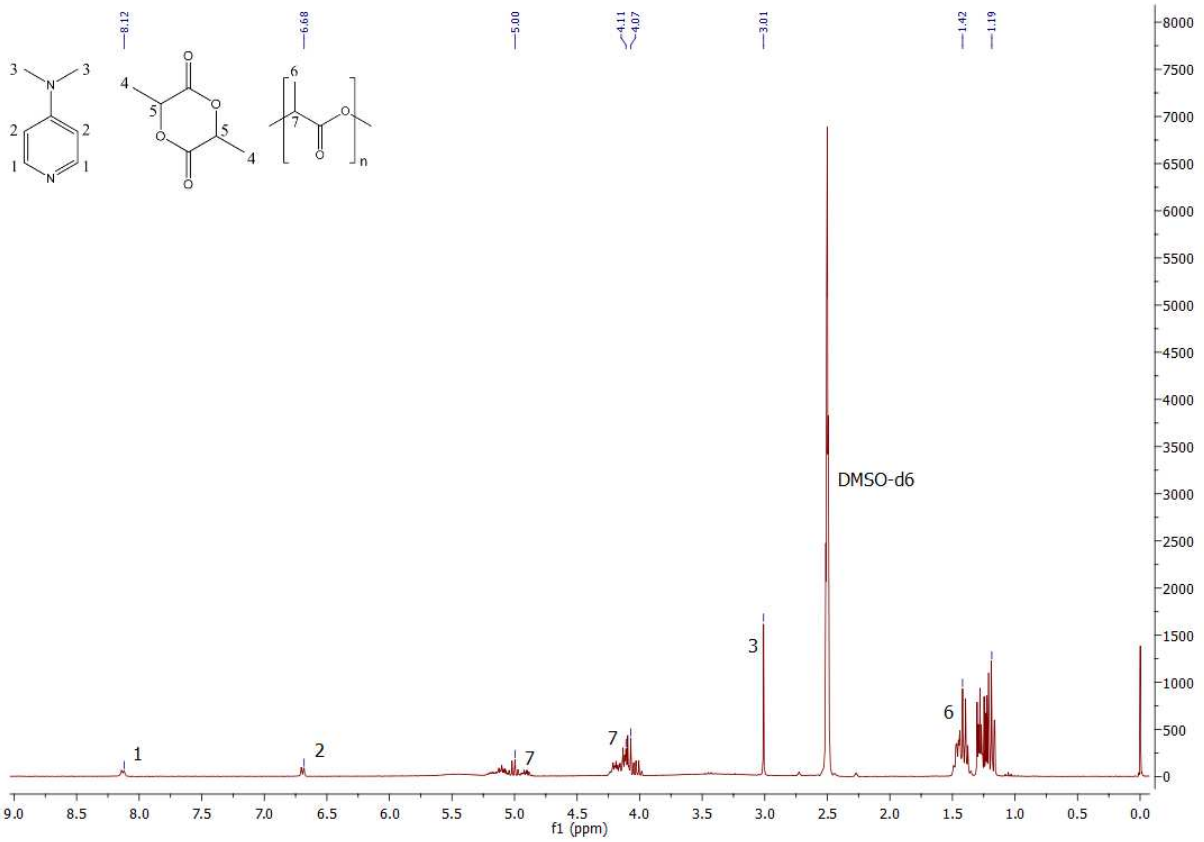


*Figure 8: 1H NMR spectra of crude mixture after reaction in DMSO-d6. Corresponds to entry 15 in table 3 (table 2 in the main manuscript)*

$^{1}$H NMR (DMSO-d6, 300 MHz) δ (ppm) 8.12 (d, 2H), 6.68 (d, 2H), 4.86-5.22 (m, 1H), 4.10-4.23 (m, 1H), 3.01 (s, 6H), 1.16-1.49 (m, 3H)

## S6. XPS Data

| | Orbital | Component | Binding energy (eV) | FWHM (eV) | % Area |
|---|---|---|---|---|---|
| *Unmodified CNF* | C 1s | C-C | 285.00 | 1.13 | 4.21 |
| | | C-O | 286.86 | 1.13 | 76.81 |
| | | O-C-O | 288.32 | 1.13 | 17.86 |
| | | O=C-O | 289.48 | 1.13 | 1.13 |
| | O 1s | O-C | 533.06 | 1.36 | 59.88 |
| | | O-C-O | 533.36 | 1.36 | 40.12 |

| | Orbital | Component | Binding energy (eV) | FWHM (eV) | % Area |
|---|---|---|---|---|---|
| *1-91-1* | C 1s | C-C | 285.00 | 1.11 | 10.68 |
| | | C-O | 286.50 | 1.11 | 69.63 |
| | | O-C-O | 287.91 | 1.11 | 16.48 |
| | | O=C-O | 289.20 | 1.11 | 3.21 |
| | O 1s | O-C | 532.89 | 1.41 | 95.05 |
| | | O-C=O | 534.05 | 1.41 | 4.95 |

| | Orbital | Component | Binding energy (eV) | FWHM (eV) | % Area |
|---|---|---|---|---|---|
| *1-91-2* | C 1s | C-C | 285.00 | 1.16 | 7.20 |
| | | C-O | 286.62 | 1.16 | 70.19 |
| | | O-C-O | 288.02 | 1.16 | 17.16 |
| | | O=C-O | 289.46 | 1.16 | 5.45 |
| | O 1s | O-C | 532.92 | 1.41 | 92.08 |
| | | O-C=O | 534.15 | 1.41 | 7.92 |

| | Orbital | Component | Binding energy (eV) | FWHM (eV) | % Area |
|---|---|---|---|---|---|
| *1-91-3* | C 1s | C-C | 285.00 | 1.18 | 5.99 |
| | | C-O | 286.46 | 1.18 | 67.89 |
| | | O-C-O | 287.82 | 1.18 | 18.53 |
| | | O=C-O | 289.36 | 1.18 | 7.59 |
| | O 1s | O-C | 532.72 | 1.41 | 88.39 |
| | | O-C=O | 534.00 | 1.41 | 11.61 |

| | Orbital | Component | Binding energy (eV) | FWHM (eV) | % Area |
|---|---|---|---|---|---|
| *1-91-4* | C 1s | C-C | 285.00 | 1.18 | 6.13 |

| | | | | | |
|---|---|---|---|---|---|
| | | C-O | 286.40 | 1.18 | 66.59 |
| | | O-C-O | 287.76 | 1.18 | 18.79 |
| | | O=C-O | 289.31 | 1.18 | 8.49 |
| | O 1s | O-C | 532.71 | 1.40 | 87.11 |
| | | O-C=O | 533.93 | 1.40 | 12.89 |

| | Orbital | Component | Binding energy (eV) | FWHM (eV) | % Area |
|---|---|---|---|---|---|
| *1-91-5* | C 1s | C-C | 285.00 | 1.22 | 19.65 |
| | | C-O | 286.41 | 1.22 | 43.41 |
| | | O-C-O | 287.45 | 1.22 | 18.12 |
| | | O=C-O | 289.16 | 1.22 | 18.83 |
| | O 1s | O-C | 532.52 | 1.43 | 70.38 |
| | | O-C=O | 533.74 | 1.43 | 29.62 |

| | Orbital | Component | Binding energy (eV) | FWHM (eV) | % Area |
|---|---|---|---|---|---|
| *1-91-6* | C 1s | C-C | 285.00 | 1.15 | 23.59 |
| | | C-O | 286.37 | 1.15 | 28.41 |
| | | O-C-O | 287.17 | 1.15 | 22.64 |
| | | O=C-O | 289.04 | 1.15 | 25.37 |
| | O 1s | O-C | 532.38 | 1.38 | 59.43 |
| | | O-C=O | 533.60 | 1.38 | 40.57 |

| | Orbital | Component | Binding energy (eV) | FWHM (eV) | % Area |
|---|---|---|---|---|---|
| *1-91-7* | C 1s | C-C | 285.00 | 1.18 | 21.79 |
| | | C-O | 286.39 | 1.18 | 35.67 |
| | | O-C-O | 287.25 | 1.18 | 18.76 |
| | | O=C-O | 289.02 | 1.18 | 23.77 |
| | O 1s | O-C | 532.41 | 1.40 | 63.06 |
| | | O-C=O | 533.63 | 1.40 | 36.94 |

| | Orbital | Component | Binding energy (eV) | FWHM (eV) | % Area |
|---|---|---|---|---|---|
| *1-91-8* | C 1s | C-C | 285.00 | 1.18 | 21.96 |
| | | C-O | 286.34 | 1.18 | 33.61 |

| | | | | | |
|---|---|---|---|---|---|
| | | O-C-O | 287.22 | 1.18 | 21.48 |
| | | O=C-O | 289.04 | 1.18 | 22.94 |
| | O 1s | O-C | 532.42 | 1.41 | 63.45 |
| | | O-C=O | 533.64 | 1.41 | 36.55 |

| | Orbital | Component | Binding energy (eV) | FWHM (eV) | % Area |
|---|---|---|---|---|---|
| *Entry 4* | C 1s | C-C | 285.00 | 1.14 | 10.57 |
| | | C-O | 286.76 | 1.14 | 70.08 |
| | | O-C-O | 288.19 | 1.14 | 16.56 |
| | | O=C-O | 289.44 | 1.14 | 2.79 |
| | O 1s | O-C | 532.97 | 1.41 | 59.30 |
| | | O-C-O | 533.27 | 1.41 | 39.73 |
| | | O-C=O | 533.77 | 1.41 | 0.49 |
| | | O-C=O | 532.37 | 1.41 | 0.49 |

| | Orbital | Component | Binding energy (eV) | FWHM (eV) | % Area |
|---|---|---|---|---|---|
| *Entry 12* | C 1s | C-C | 285.00 | 1.12 | 9.12 |
| | | C-O | 286.80 | 1.12 | 71.63 |
| | | O-C-O | 288.23 | 1.12 | 16.94 |
| | | O=C-O | 289.57 | 1.12 | 1.83 |
| | O 1s | O-C | 533.00 | 1.37 | 59.53 |
| | | O-C-O | 533.30 | 1.37 | 39.89 |
| | | O-C=O | 533.80 | 1.37 | 0.29 |
| | | O-C=O | 532.40 | 1.37 | 0.29 |

| | Orbital | Component | Binding energy (eV) | FWHM (eV) | % Area |
|---|---|---|---|---|---|
| *Entry 15* | C 1s | C-C | 285.00 | 1.13 | 6.21 |
| | | C-O | 286.75 | 1.13 | 72.85 |
| | | O-C-O | 288.15 | 1.13 | 17.06 |
| | | O=C-O | 289.41 | 1.13 | 3.01 |
| | O 1s | O-C | 532.95 | 1.38 | 59.26 |
| | | O-C-O | 533.25 | 1.38 | 39.71 |
| | | O-C=O | 533.75 | 1.38 | 0.52 |

| | | | | |
|---|---|---|---|---|
| | O-C=O | 532.35 | 1.38 | 0.52 |